Journal of the Serbian Chemical Society
JSCS-info@shd.org.rs • www.shd.org.rs/JSCS
J. Serb. Chem. Soc. 82 (3) 379–390 (2017)
JSCS–5081
UDC 66.011+66.087.3:510.644:575.113
Original scientific paper

Modelling and optimizing an electrochemical oxidation process using artificial neural network, genetic algorithm and particle swarm optimization

BANGHAI LIU, CHUNJI JIN*, JITENG WAN, PENGFANG LI and HUANXI YAN

College of Environmental Science and Engineering, Ocean University of China, No. 238 Songling Road, Qingdao, Shandong Province 266100, China

(Received 21 July, revised 8 September, accepted 12 September 2017)

Abstract: This study proposes a novel hybrid of artificial neural network (ANN), genetic algorithm (GA), and particle swarm optimization (PSO) to model and optimize the relevant parameters of an electrochemical oxidation (EO) Acid Black 2 process. The back propagation neural network (BPNN) was used as a modelling tool. To avoid over-fitting, GA was applied to improve the generalized capability of BPNN by optimizing the weights. In addition, an optimization model was developed to assess the performance of the EO process, where total organic carbon (*TOC*) removal, mineralization current efficiency (*MCE*), and the energy consumption per unit of TOC (EC_{TOC}) were considered. The operation conditions of EO were further optimized *via* PSO. The validation results indicted the proposed method to be a promising method to estimate the efficiency and to optimize the parameters of the EO process.

Keywords: electrochemical oxidation; artificial neural network; genetic algorithm; particle swarm optimization, Acid Black 2.

INTRODUCTION

Electrochemical oxidation (EO) is one of the most promising advanced oxidation processes (AOPs) that has been widely used for the treatment of industrial wastewater, contaminated groundwater, and hazardous waste due to its energy efficiency, usefulness, and environmental friendliness.[1–5] *Via* EO, a large number of active substances (mainly hydroxyl radicals, $^{\bullet}OH$) are produced, which can both directly and indiscriminately react with contaminants, and mineralize pollutants into CO_2, H_2O, or simple intermediates without secondary pollution.[6–8] Therefore, the application of electrochemical technologies can provide an alternative to treat wastewaters containing biological toxicity and resistant substances,

* Corresponding author. E-mail: liubanghai2017@163.com
https://doi.org/10.2298/JSC170721101L

which conventional methods cannot properly dispose of (*e.g.*, pharmaceutical wastewater, industrial dye wastewater, or municipal solid waste leachate).[9–11]

Currently, numerous studies are devoted to analyzing the effects of electrode material, pollutant parameters, and aqueous conditions on an EO system and have attained plenty of valuable results.[12–15] However, the study of modelling and optimizing the EO process has always been neglected, despite this being a critical step for the practical application of electrochemical technology. According to the previous research, the performance of EO is related to many operating variables such as applied current density, electrolyte, pH, and electrolysis time.[16] Therefore, it is difficult to model a process with multiple variables. Fortunately, Artificial neural network (ANN) provides a new way to solve this complicate problem.

ANN is powerful modelling tool with both the ability and flexibility to model any complex and non-linear phenomenon, especially in multivariate calibration.[17] Due to the unique capability of learning, simulation, and predicting of date, ANN has been commonly employed in many areas of science and engineering.[18–20] Moreover, in order to assist designers to discern optimal related operating parameters, it is necessary to select and utilize some appropriate optimization methods. Genetic algorithm (GA) and particle swarm optimization (PSO) are two widely used evolutionary algorithms that have been combined with ANN. GA is an adaptive heuristic algorithm, inspired by the natural selection and the genetics including population, crossover, and mutation steps.[21] GA can directly work with structural objects without the requirement of derivation and the restriction of function continuity. Furthermore, through the adoption of probabilistic optimization methods, GA is able to automatically obtain and guide an optimized search space and adaptively adjust the search direction. Accordingly, in comparison with conventional methods, GA represents the superior practicality and compatibility. PSO is based on the idea of simulating bird predation behaviour and it is a new algorithm developed during recent years. PSO starts from a random solution and searches the optimal solution via iteration. The global optimal is sought by following the optimal value among those currently searched and the quality of the solution is evaluated via fitness. Recently, PSO has attracted the considerable attention due to its characteristics of simple algorithm, high precision, and fast convergence. In contrast to GA, PSO has the advantage that it is easy to implement and requires only few parameters to adjust; however, it bears the risk of falling into the local optimal.

The objective of this study was to exploit the ANN to model the process of EO synthesis of dye wastewater and to optimize the relevant parameters via GA and PSO. Additionally, the construction, training, and optimization of ANN was also investigated in detail to acquire a better understanding of ANN.

EXPERIMENTAL

Reagents and materials

A handcrafted PbO_2 anode and stainless-steel (SS304) cathode were selected as electrodes with dimensions of 10 cm (length)×8 cm (width). All chemicals, including sodium chloride, sodium hydroxide, sulphuric acid, and Acid Black 2 were of analytical grade. All solutions were prepared with double deionised water (Mill-Q^{TM} system, resistivity = 18 MΩ cm at 25 °C).

Experimental procedure

The experimental setup consisted of an electrolytic cell (1000 mL), electrodes, a DC power supply (KXN-305D), and a magnetic stirrer. For each experiment, the electrolytic cell contained AB2 and sodium chloride (electrolyte), dissolved by deionised water with electrodes, was soaked in solution. A solution of 0.01 M sodium hydroxide/sulphuric acid was used to adjust the pH of the electrolyte solution. Experiments were conducted under galvanostic conditions at 25 °C with a stirring speed of 350 rpm. Samples were collected every 10 min to measure TOC (TOC-VCPN analyzer) during a 60-min experiment.

Artificial neural network (ANN)

Data set. To reduce the number of experiments, while obtaining more useful information, the response surface methodology, based on central composite design, was employed as experimental design method.[22] The independent variable levels were: AB2 concentration (300–600 mg L^{-1}), current density (5–10 mA cm^{-2}), electrolyte (0.05–0.15 mg L^{-1}), and pH (4––10). According to the design matrix, a total 30 experiments were conducted, ultimately yielding 210 sets of data that were used to construct the ANN.

Optimization model. To evaluate the performance of the EO process, *TOC* removal, mineralization current efficiency (*MCE*), and energy consumption per unit *TOC* (EC_{TOC}) were taken into account. A developed optimization model was applied to quantify the properties of the EO process. The terms of the model are shown in Eq. (1):

$$Y = W_1a + W_2c + W_3(1–c) \tag{1}$$

In the objective function, the values of *a*, *b* and *c* represent *TOC* removal, *MCE* and EC_{TOC}, respectively. In addition, *a*, *b*, and *c* were the normalized variables in the range of 0–1 *via* min–max normalization. The lower the energy consumption, the higher the value 1–*c*. Since the most significant objective for this study was to removal *TOC*, W_1 was set to 0.8, whileW_2 and W_3 were set to 0.1. This indicated the purpose of reaching maximum *TOC* removal with a logical compromise among efficiency and cost.

The values of *MCE* and EC_{TOC} were calculated based on Eqs. (2) and (3), respectively:[23–27]

$$MCE, \% = 100\frac{nFV(TOC_t - TOC_{t+\Delta t})}{4.23\times10^7 mIt} \tag{2}$$

$$EC_{TOC}, \text{kWh g}^{-1} = \frac{E_{\text{cell}}It}{V(TOC_t - TOC_{t+\Delta t})} \tag{3}$$

where TOC_t and $TOC_{t+\Delta t}$ are the total organic carbon at times *t* and $t+\Delta t$ (s). *I* is the applied current (A), E_{cell} is the applied voltage (V), *t* is the reaction time in the reactor (h), *V* is the volume of the reactor (L), *F* is the Faraday constant (96485 C mol^{-1}), 4.23×10^7 is a conversion factor, *m* is the number of carbon atoms of AB2, *n* is the number of consumed

electrons per AB2 molecule, and *n* and *m* were fixed at 36 and 137, respectively, according to Eq. (4):

$$C_{36}H_{28}N_5O_6Na_2 + 66H_2O \rightarrow 36CO_2 + 5NH_4^+ + 140H^+ + 2Na^+ + 137e^- \quad (4)$$

Back propagation neural network combined with GA and PSO (GA-BPNN-PSO). Back propagation neural network (BPNN), one of the most widespread used ANN models that was applied in modelling the EO process via a neural network toolbox in MATLAB software (MATLAB-R2012b). Basically, the ANN structure was composed of an input layer, a hidden layer, and an output layer. The number of neurons in each layer was decided by the nature of the practical problems. In the present study, there were five neurons in the input layer (AB2 concentration, current density, electrolyte, pH and time) and the result of the optimization model (*Y*) was the neuron in the output layer. Due to the danger of the easily over-fitting BPNN, GA was used to improve the generalized ability via optimizing the initial weights of BPNN. Furthermore, PSO was applied to optimize pertinent parameters to obtain a more efficient EO process. The algorithm flow is shown in Fig. 1.

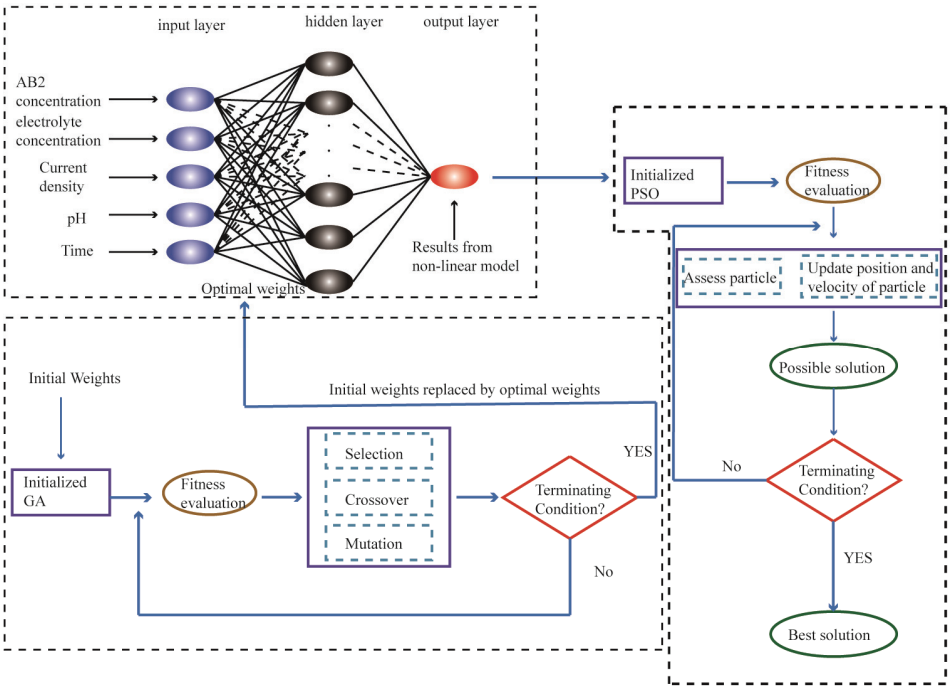

Fig. 1. Flowchart of the BPNN in combination with GA and PSO. Fitness of GA is the error between predicted values and experimental data, while fitness of PSO is the output of BPNN.

RESULTS AND DISCUSSION

BPNN modelling

In this study, randomly selected 200 sets of data were used to prepare and develop BPNN, while the rest of the 10 sets of data were used to test it. The

training data set was used to adjust the weights on the neural network and the test data set was used only for testing the final solution in order to confirm the actual predictive. The root mean square error (*RMSE*), the coefficient of determination (R^2), and the absolute average deviation (*ADD*) were applied to evaluate the fitting accuracy of BPNN. Theoretically, the activation function (AF), train function (TF), and the number of neurons of the hidden layer all have a considerable impact on the accuracy of BPNN.

The role of the AF was to distribute the independent variables in the input layers over the hidden layers and to feed the results of neurons of hidden layers into the output layer. *Via* adjusting the weight and the bias of each neuron with TF, the predictive ability of the neural network can be achieved.[28] The logarithmic sigmoid, symmetric sigmoid, and linear functions are the most commonly used AF in BPNN. Furthermore, the different combinations of *AF* would lead to completely different consequences.[29] The results displayed in Table I suggest that the sigmoid function in the hidden layer and the linear function in the output layer were the optimal combination with minimum values for *ADD* and *RMSE* of 1.77% and 0.22, respectively.

TABLE I. Values of ADD and RMSE of the different combinations of AF in BPNN during training stage

AF in hidden layer	AF in output layer	*ADD* / %	*RMSE*
Logarithmic sigmoid	Linear	1.77	0.22
Logarithmic sigmoid	Symmetric sigmoid	10.00	1.00
Logarithmic sigmoid	Logarithmic sigmoid	31.14	5.92
Symmetric sigmoid	Symmetric sigmoid	4.23	0.73
Symmetric sigmoid	Logarithmic sigmoid	5.76	0.89
Symmetric sigmoid	Linear	1.84	0.23
Linear	Logarithmic sigmoid	19.24	2.52
Linear	Symmetric sigmoid	2.24	0.29
Linear	Linear	2.05	0.26

Empirically, the number of neurons of the hidden layer depends on the input–output construction. With the increasing number of neurons, the performance of BPNN would deteriorate after an improving trend. Furthermore, it is vital to employ an appropriate algorithm, which was used to adjust the weight and the bias of each neuron. In this work, the BPNN was further trained using the algorithm of gradient descent backpropagation (traingd), gradient descent with momentum (traingdm), gradient descent with adaptive lr backpropagation (traingda), gradient descent momentum and an adaptive lr backpropagation (traingdx), and the Levenberg–Marquardt backpropagation (trainlm). As shown in Fig. 2, apparently, trainlm's performance was better than other train algorithm. In addition, increasing the number of neurons more than 11 did not significantly decrease the

RMSE. Thus the optimal obtained BPNN for modelling the EO process has the structure of 5-11-1 with trainlm as BP algorithm.

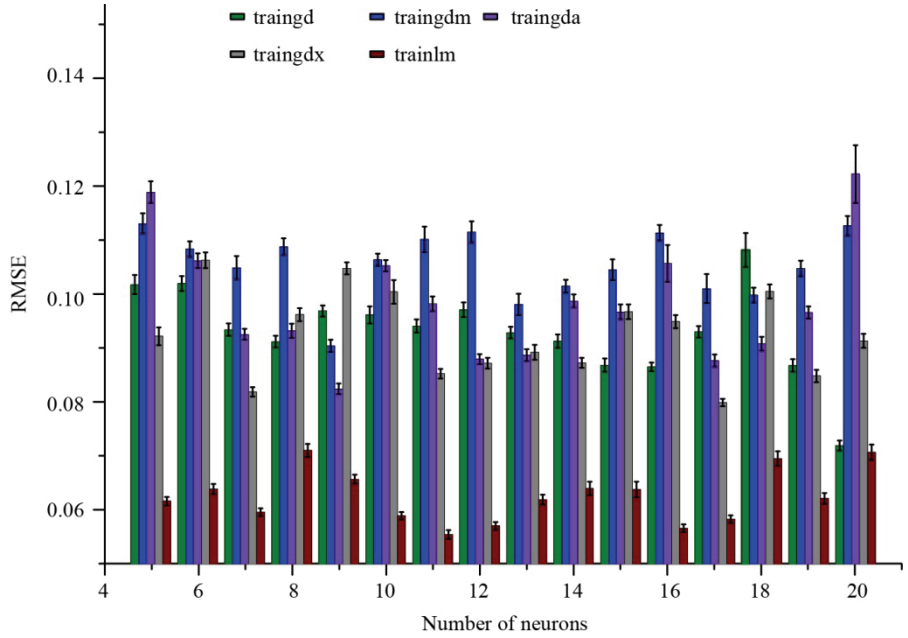

Fig.2. The *RMSE* accuracies of each algorithm during training stage.

BPNN based on GA (GA-BPNN)

Although the developed BPNN can be utilized to model the EO process with an acceptable accuracy, the simulation performance could be further improved via GA. GA is a type of heuristic optimization method, where various complex structures are represented by using simple coding techniques and the learning and search directions are determined by the genetic operations, including population, crossover, and mutation. The value of individual fitness is the standard that decides the possibility of genetic opportunities. In the current study, the error between predicted values and experimental data was considered as fitness. GA was used to replace the conventional learning algorithm to quickly and accurately obtain the best weights and bias of neurons. The predefined parameters of GA were as follows: The crossover rate and the mutation rate were set to 0.6 and 0.03, respectively; the number of generations was 30 and the size of the population was set to 20.

Tables II and III list the optimal weights and bias of BPNN and GA-BPNN. *Via* calculating the weights and bias, the relative importance of the independent variable on the response can be concluded, suggesting that the initial AB2 concen-

TABLE II. Matrices of weights and bias of BPNN, W_1: weights between input and hidden layers, W_2: weights between hidden and output layers, B_1: bias between input and hidden layers, B_2: bias between hidden and output layers, c_0: initial AB2 concentration, j: current density, c_{e0}: electrolyte concentration

W_1	Input					B_1	W_2	Output
Neuron	Variable						Neuron	Y
	c_0 /mg L^{-1}	j / mA cm^{-2}	pH	c_{e0} / mg L^{-1}	Time, min			
1	–0.882	–0.265	0.498	–0.676	0.529	–1.317	1	–0.119
2	0.342	–0.913	0.655	0.485	0.468	–0.893	2	–0.378
3	0.331	–1.011	0.826	–0.625	1.010	2.646	3	–0.227
4	–0.606	–0.845	–0.652	–0.754	0.804	2.517	4	0.156
5	0.730	–0.403	0.935	–0.722	0.538	2.720	5	–0.211
6	–0.836	–0.378	0.875	0.123	0.080	–1.250	6	0.605
7	–0.933	–0.364	–0.558	–0.275	–0.732	0.990	7	–0.337
8	–0.812	0.176	0.706	–0.723	0.356	–2.286	8	0.362
9	0.826	–0.247	–0.741	–0.106	–0.186	–2.141	9	0.590
10	0.193	–0.337	0.897	–0.189	0.490	–2.278	10	0.843
11	0.648	0.477	–0.916	0.100	0.922	2.048	11	0.256
							B_2	0.537

TABLE III. Matrices of weights and bias of GA-BPNN, W_1: weights between input and hidden layers, W_2: weights between hidden and output layers, B_1: bias between input and hidden layers, B_2: bias between hidden and output layers, c_0: initial AB2 concentration, j: current density, c_{e0}: electrolyte concentration

W_1	Input					B_1	W_2	Output
Neuron	Variable						Neuron	Y
	c_0 / mg L^{-1}	j / mA cm^{-2}	pH	c_{e0} / mg L^{-1}	Time, min			
1	–2.077	–1.555	–1.966	–1.767	–2.073	–0.119	1	–0.687
2	–1.833	–1.227	1.574	2.461	0.972	–0.378	2	–2.526
3	–0.609	–2.691	2.288	0.685	2.704	–0.227	3	–0.688
4	–2.276	2.618	0.487	–2.074	2.098	0.156	4	–1.902
5	0.974	1.278	2.121	1.935	0.996	–0.211	5	–2.414
6	0.281	–2.472	1.690	–0.131	–1.990	0.605	6	1.317
7	1.856	–0.336	–2.210	–1.590	2.524	–0.337	7	1.129
8	–2.457	1.981	–2.672	–1.124	0.797	0.362	8	–0.585
9	–0.078	–0.195	–2.797	–0.043	1.887	0.590	9	–0.636
10	2.871	2.152	–2.859	1.793	2.101	0.843	10	1.155
11	1.096	–1.641	–2.614	0.309	–0.758	0.256	11	–1.944
							B_2	–1.357

tration is higher than that of other factors (Table IV). The calculation equation is as follows:[30]

$$I_p = \frac{\sum_{m=1}^{Nh}\left(\left(\left|w_{pm}^{ih}\right| \Big/ \sum_{k=1}^{Ni}\left|w_{km}^{ih}\right|\right)\times\left|w_{mn}^{ho}\right|\right)}{\sum_{k=1}^{k=Ni}\left\{\sum_{m=1}^{Nh}\left(\left(\left|w_{pm}^{ih}\right| \Big/ \sum_{k=1}^{Ni}\left|w_{km}^{ih}\right|\right)\times\left|w_{mn}^{ho}\right|\right)\right\}} \quad (5)$$

where I_p is the relative importance of the p^{th} input variable on the output variable, *Ni* and *Nh* are the number of neurons in input and hidden layers, respectively. The superscripts i, h, and o represent the input, hidden and output layers. The subscripts *k*, *m*, and *n* are the input, hidden and output neurons, respectively.

TABLE IV. Relative importance of the independent parameter of BPNN and GA-BPNN

Variable	Relative importance of BPNN, %	Relative importance of GA-BPNN, %
c_0 / mg L^{-1}	28.75	23.22
j / mA cm^{-2}	15.01	18.16
pH	26.38	22.32
c_{e0} / mg L^{-1}	11.53	16.28
Time, min	18.33	20.02
Total	100.00	100.00

Evaluating the performance of BPNN and GA-BPNN

To acquire a comprehensive comparison between the two proposed models, criteria including *RMSE* and R^2 were considered. Furthermore, the simulated and predicted consequences were applied to assess the accuracy and feasibility of BPNN and GA-BPNN through a regression analysis, as shown in Figs. 3 and 4.

Regression plots indicated that the two proposed models were successful to simulate the response with adequate accuracy during the training procedure with the values of R^2 were 0.97 and 0.96, respectively. This also demonstrated that the fit quality of BPNN was even a little better than that of GA-BPNN, in accordance with values of R^2. The predictive ability of the above models were assessed by testing a set of data, which was never used in the training process.[31] Apparently, the predictive accuracy of BPNN was unsatisfactory (R^2 was 0.90), while the GA-BPNN still displayed an excellent predictive performance (R^2 was 0.97). The *RMSE* of BPNN and GA-BPNN in the test process were 0.596 and 0.248, respectively. This suggests that BPNN is an optimized method for local search, which can always be utilized to solve global optimization problems. Therefore, obtaining the local optimal solution and over-fitting are commonplace. BPNN combined with GA is a type of heuristic learning algorithm that can successfully avoid the drawback and improve the generalized capacity. However, the normal residual plots are a tool to verify the model availability. The histograms of the standardized residual and the Gaussian curve illustrate that the residuals of BPNN and GA-BPNN conformed to normal distribution for both training and test data. Such results suggest high credibility of the predicted data for both proposed models. In addition, the residuals (Fig. 5) of BPNN and GA-BPNN are randomly distributed and almost symmetrically fill the negative and positive half-planes, leading to exclude a systematic error.

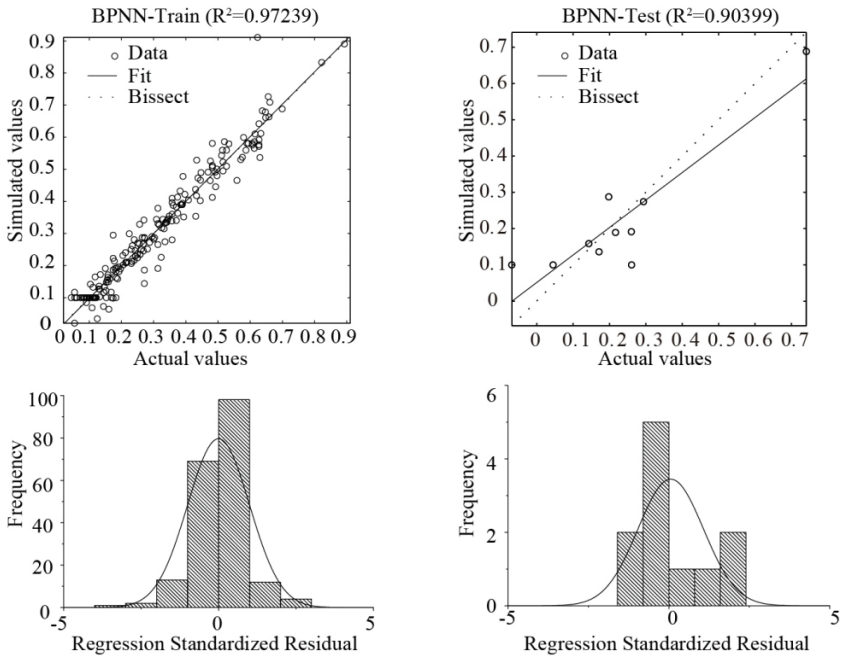

Fig. 3. Regression and normal residuals plots for training and test data of BPNN.

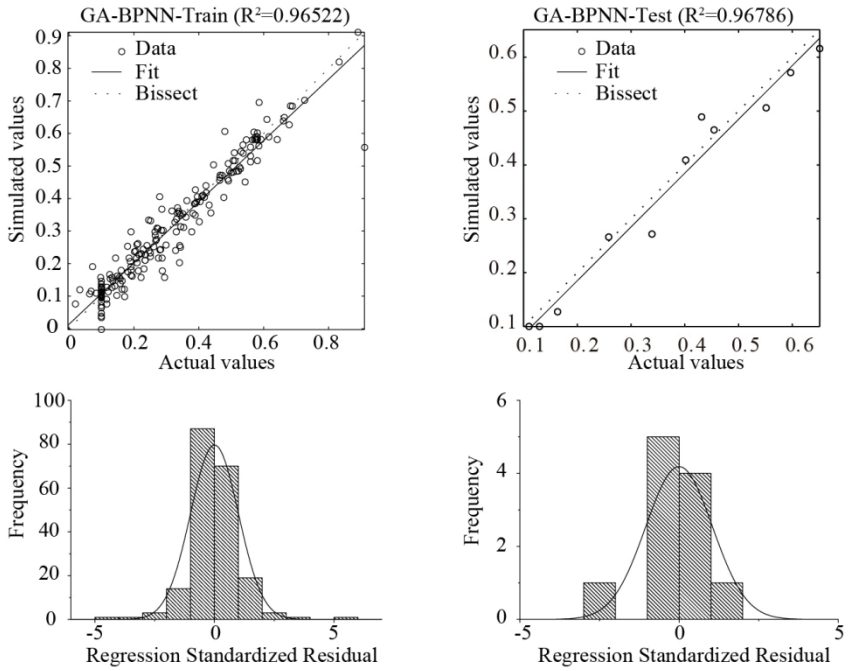

Fig. 4. Regression and normal residuals plots for training and test data of GA-BPNN.

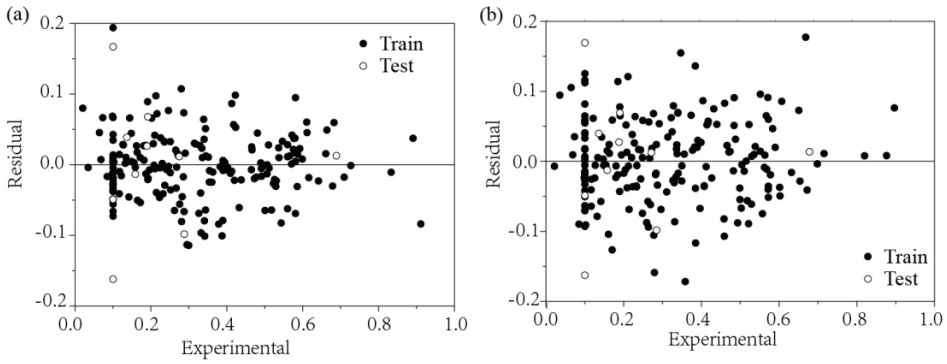

Fig. 5. Residual *vs.* experimental plots of BPNN (a) and GA-BPNN (b).

In summary, both BPNN and GA-BPNN are available for the modelling of EO processes, providing high accuracy during the training procedure; however, considering the generalized capacity (testing procedure), GA-BPNN should be preferred.

Process parameter optimization based on PSO

Theoretically, ANN can map any complex non-linear relationship due to its outstanding non-linear fitting ability. However, the apparent flaw is that it cannot provide an exact mathematical description, resulting in a huge challenge in optimizing the pertinent parameters that are involved in the process. PSO is a type of evolutionary algorithm that was inspired by the social behaviour of bird swarms in search of food.[32] Due to the advantages of the high precision, fast convergence, and ease of operation, PSO has shown superiority on several complex optimization problems, especially on the abstract function optimization.[31] In this study and for the purpose of achieving the best performance of EO, the relevant parameters were optimized *via* PSO using the design range. The predefined parameters for guiding the PSO are as follows: learning factors of 1.49445, maximum generation of 100, and population size of 20. The maximum and minimum velocities of each particle were 1 and -1, respectively. Furthermore, the predicted value from GA-BPNN was selected as the PSO fitness.

Table V lists the results of the verification experiment of an optimal solution due to PSO. The optimal parameters were readjusted to facilitate the experimental operation. The relative error between simulation and experimental validation result was 8.3 %. Furthermore, the *TOC* removal, *MCE* and EC_{TOC} were 63.3 %, 49 %, and 1.45 kWh g^{-1}, respectively. This indicted that the GA-BPNN-PSO can successfully be applied to model the process and to optimize the performance of EO with an acceptable accuracy.

TABLE V. Comparison of optimization and experimental results

Solution	c_0 / mg L^{-1}	j / mA cm^{-2}	pH	c_{e0} / mg L^{-1}	Time, min	Y
GA-BPNN-PSO	499.71	7.39	4.59	0.08	49.74	0.63
Adjusted	500.00	8.00	4.00	0.08	50.00	0.60
Experiment	500.00	8.00	4.00	0.08	50.00	0.65

CONCLUSION

This study presents a novel hybrid of BPNN, GA, and PSO for modelling and optimizing the related parameters of an EO process. The effects of AB2 concentration, current density, electrolyte, pH, and time on the performance of EO were assessed via non-linear model, considering *TOC* removal, *MCE* and EC_{TOC}. The topology of BPNN was composed of an input layer, a hidden layer, and an output layer. For each layer, the number of neurons was 5, 11, and 1, respectively, using Levenberg–Marquardt backpropagation as the training function. Compared with the results of BPNN and GA-BPNN, it was concluded that GA can further improve the generalized capacity of BPNN through optimizing both weights and bias. The achieved relative importance of independent parameters on the quality of EO suggested the electrolyte concentration as the most significant influencing factor on the quality of EO. According to the optimal parameters derived from PSO, a *TOC* removal of 63.3 %, an *MCE* of 49 % and an EC_{TOC} of 1.45 kWh g^{-1} were achieved. The validation results are comparable to the solution generated *via* PSO. The proposed method can be utilized to both model and optimize the EO process to design more efficient EO-based water disposal units.

ИЗВОД

МОДЕЛОВАЊЕ И ОПТИМИЗАЦИЈА ПРОЦЕСА ЕЛЕКТРОХЕМИЈСКЕ ОКСИДАЦИЈЕ ACID BLACK 2 БОЈЕ КОРИШЋЕЊЕМ ВЕШТАЧКЕ НЕУРОНСКЕ МРЕЖЕ, ГЕНЕТИЧКОГ АЛГОРИТМА И ОПТИМИЗАЦИЈЕ РОЈА ЧЕСТИЦА

BANGHAI LIU, CHUNJI JIN, JITENG WAN, PENGFANG LI и HUANXI YAN

[1]*College of Environmental Science and Engineering, Ocean University of China, No. 238 Songling Road, Qingdao, Shandong Province 266100, China*

Ова студија предлаже нови хибрид вештачке неуронске мреже (ANN), генетичког алгоритма (GA) и оптимизације роја честица (PSO) у моделовању релевантних параметара процеса електрохемијске оксидације (EO) боје Acid Black 2. Архитектура са пропагацијом грешке уназад (BPNN) је коришћена за развој модела. Да би се избегла претренираност и побољшала генерализација BPNN модела, примењен је GA за оптимизацију тежинских коефицијената. Додатно је развијен и оптимизациони модел за процену ефикасности самог EO процеса, при чему су оптимизовани уклањање *TOC*, ефикасност струје минерализације и потрошња енергије по јединици уклоњеног *TOC*. Оптимизација самог процеса је вршена PSO алгоритмом. Резултати су показали да предложени приступ даје задовољавајуће резултате код предвиђања ефикасности и оптимизације параметара EO процеса.

(Примљено 21. јула, ревидирано 8. септембра, прихваћено 12. септембра 2017)

REFERENCES

1. H. Li, Z. Shi, C. Zhu, *Croat. Chem. Acta* **87** (2014) 185
2. A. Y. Bagastyo, J. Radjenovic, Y. Mu, R. A. Rozendal, D. J. Batstone, K. Rabaey, *Water. Res.* **45** (2011) 4951
3. A. Butkovskyi, A. W. Jeremiasse, L. Hernandez Leal, T. van der Zande, H. Rijnaarts, G. Zeeman, *Environ. Sci. Technol.* **48** (2014) 1893
4. B. P. Chaplin, *Environ. Sci. – Proc. Imp.* **16** (2014) 1182
5. J. Radjenovic, D. L. Sedlak, *Environ. Sci. Technol.* **49** (2015) 11292
6. G. Chen, *Sep. Purif. Technol.* **38** (2004) 11
7. B. Yang, P. Geng, G. Chen, *Sep. Purif. Technol.* **156** (2015) 931
8. Q. Dai, J. Zhou, M. Weng, X. Luo, D. Feng, J. Chen, *Sep. Purif. Technol.* **166** (2016) 109
9. X. Quan, Z. Cheng, B. Chen, X. Zhu, *J. Environ. Sci. – China* **25** (2013) 2023
10. M. M. Cid-Cerón, D. S. Guzmán-Hernández, M. T. Ramírez-Silva, A. Galano, M. Romero-Romo, M. Palomar-Pardavé, *Electrochim. Acta.* **199** (2016) 92
11. G. Ramírez, F. J. Recio, P. Herrasti, C. Ponce-de-León, I. Sirés, *Electrochim. Acta* **204** (2016) 9
12. C. Comninellis, C. Pulgarin, *J. App. Electrochem.* **23** (1993) 108
13. H. Li, X. Zhu, Y. Jiang, J. Ni, *Chemosphere* **80** (2014) 845
14. R. E. Palma-Goyes, F. L. Guzmán-Duque, G. Peñuela, I. González, J. L. Nava, R. A. Torres-Palma, *Chemosphere* **81** (2010) 26
15. L. Labiadh, A. Barbucci, M. P. Carpanese, A. Gadri, S. Ammar, M. Panizza, *J. Appl. Electrochem.* **766** (2016) 94
16. H. Li, X. Zhu, J. Ni, *Electrochim. Acta* **56** (2010) 448
17. F. Geyikçi, E. Kılıç, S. Çoruh, S. Elevli, *Chem. Eng. J.* **183** (2012) 53
18. M. Mohajerani, M. Mehrvar, F. Ein-Mozaffari, *Chem. Prod. Process. Model.* **6** (2011) 1
19. J. S. Ahari, M. T. Sadeghi, S. Zarrinpashne, A. Irandoukht, *Sci. Iran.* **20** (2013) 617
20. S. Azadi, H. Amiri, G. R. Rakhshandehroo, *Waste Manage.* **55** (2016) 220
21. N. Biglarijoo, S. A. Mirbagheri, M. Bagheri, M. Ehteshami, *Process. Saf. Environ.* **106** (2016) 89
22. V. A. Sakkas, M. A. Islam, C. Stalikas, T. A. Albanis, *J. Hazard. Mater.***175** (2010) 33
23. V. K. Pareek, M. P. Brungs, A. A. Adesina, R. Sharma, *J. Photochem. Photobiol., A* **149** (2002) 139
24. L. C. Almeida, S. Garcia-Segura, N. Bocchi, E. Brillas, *Appl. Catal., B: Environ.* **103** (2011) 21
25. E. J. Ruiz, C. Arias, E. Brillas, A. Hernández-Ramírez, J. M. Peralta-Hernández, *Chemosphere* **82** (2011) 495
26. R. Salazar, S. Garcia-Segura, M. S. Ureta-Zañartu, E. Brillas, *Electrochim. Acta* **56** (2011) 6371
27. W. Khongthon, G. Jovanovic, A. Yokochi, P. Sangvanich, V. Pavarajarn, *Chem. Eng. J.* **292** (2016) 298
28. K. V. Gernaey, M. C. van Loosdrecht, M. Henze, M. Lind, S. B. Jørgensen, *Environ. Modell. Software* **19** (2004) 763
29. A. Wu, Z. Zeng, C. Fu, W. Shen, *Neurocomputing* **74** (2011) 831
30. G. D. Garson, *AI Expert* **6** (1991) 46
31. M. R. Tanweer, R. Auditya, S. Suresh, N. Sundararajan, N. Srikanth, *Swarm. Evol. Comput.* **28** (2016) 98
32. A. Benvidi, S. Abbasi, S. Gharaghani, M. D. Tezerjani, S. Masoum, *Food. Chem.* **220** (2017) 377.